HHS Public Access

Author manuscript

Proc SPIE Int Soc Opt Eng. Author manuscript; available in PMC 2009 July 14.

Published in final edited form as:

Proc SPIE Int Soc Opt Eng. 2009 ; 7161: 71612G. doi:10.1117/12.813087.

Fluorescence lifetime imaging microscopy for the characterization of atherosclerotic plaques

Jennifer Phipps[a], **Yinghua Sun**[a,b], **Ramez Saroufeem**[c], **Nisa Hatami**[a], and **Laura Marcu**[a,b]

[a]Department of Biomedical Engineering University of California, Davis, California

[b]NSF Center for Biophotonics University of California, Davis, California

[c]Department of Medical Pathology and Laboratory Medicine University of California, Davis, California

Abstract

Atherosclerotic plaque composition has been associated with plaque instability and rupture. This study investigates the use of fluorescence lifetime imaging microscopy (FLIM) for mapping plaque composition and assessing features of vulnerability. Measurements were conducted in atherosclerotic human aortic samples using an endoscopic FLIM system (spatial resolution of 35 μm; temporal resolution 200 ps) developed in our lab which allows mapping in one measurement the composition within a volume of 4 mm diameter × 250 μm depth. Each pixel in the image represents a corresponding fluorescence lifetime value; images are formed through a flexible 0.6 mm side-viewing imaging bundle which allows for further intravascular applications. Based on previously recorded spectra of human atherosclerotic plaque, fluorescence emission was collected through two filters: f1: 377/50 and f2: 460/60 (center wavelength/bandwidth), which together provides the greatest discrimination between intrinsic fluorophores related to plaque vulnerability. We have imaged nine aortas and lifetime images were retrieved using a Laguerre expansion deconvolution technique and correlated with histopathology. Early results demonstrate discrimination using fluorescence lifetime between early, lipid-rich, and collagen-rich lesions which are consistent with previously reported time-resolved atherosclerotic plaque measurements.

Keywords

atherosclerotic plaque; fluorescence lifetime imaging microscopy (FLIM); time-resolved fluorescence; endoscopy

1. INTRODUCTION

Cardiovascular disease remains the number one cause of death in developed nations and myocardial infarction caused by atherosclerosis is a major contributor to the cardiovascular death toll every year. Despite the shift in understanding of atherosclerosis from a “plumbing problem” to a more complex process independent of vessel stenosis, current diagnostic methods which mainly rely on plaque size rather than composition are inadequate[1]. Many

new modalities are being investigated as potential methods of diagnosing “vulnerable” plaques[2], in particular the thin-cap fibroatheroma which consists of a thin fibrous cap (<65 μm) covering a large lipid core[3]. Time resolved fluorescence imaging is a feasible means of tissue diagnosis in general because of its ability to resolve overlapping spectra of endogenous fluorophores, its independence from fluorophore concentration and fluorescence intensity, and its sensitivity to pH and other environmental parameters[4]. It is well-suited for recognizing markers of plaque vulnerability because of the endogenous fluorophores it can resolve that are related to plaque composition such as lipids, collagen, and elastin[5]. Previous work in our lab has shown time resolved fluorescence spectroscopy capable of recognizing markers of plaque vulnerability in human carotid and aortic plaque[6-8] and macrophages in a rabbit model[9]. This work aims to build on our previous work by providing a method of correlating fluorescence lifetime imaging microscopy (FLIM) images of ex vivo, intact human cadaver aortic plaques with histopathological information to characterize the chemical composition particularly related to plaque vulnerability.

2. METHODS

2.1 Tissue methodology

Human aorta samples were received post-mortem and frozen within 2 hours from autopsy. They were snap-frozen by first being dipped in isopentane to reduce freezing artifacts then dipped in liquid nitrogen and stored at -80 degrees Celsius. The samples were defrosted at 2-3 degrees Celsius overnight before being imaged.

2.2 FLIM methodology

This system allows mapping in one measurement the composition within a volume of 4 mm diameter × 250 μm depth with ∼35 μm spatial and ∼200 ps temporal resolution. A series of fluorescence images encompassing the fluorescence decay in 0.5 ns time intervals is formed through a flexible 0.6 mm imaging bundle (10,000 coherent fibers with a GRIN objective lens and 90 degree prism for side-viewing). This imaging bundle is comparable in size to angioscopes used for heart catheterizations, allowing for the potential of this probe to be used intravascularly. Each pixel in the image series represents a fluorescence decay curve from one ∼35 μm area on the sample. Based on previous spectroscopic results from human atherosclerotic plaque measured in our lab[6], two filters were used: f1: 377/50 and f2: 460/60 (center wavelength/bandwidth), which together provides the greatest discrimination between intrinsic fluorophores related to plaque vulnerability. Each image series was recorded in ∼2.5 minutes and the specimens were kept moist with drops of saline during the imaging process. Currently, 40 different locations (80 series of images including f1 and f2) have been imaged between nine aortas. The location of the FLIM measurements were marked with India ink following imaging and the samples were sent for histopathological analysis.

2.1 FLIM Data Analysis

The fluorescence response is retrieved from each series of FLIM images through deconvolution with a Laguerre expansion technique[10] implemented by a graphical user interface written in MATLAB. During the pixel by pixel deconvolution process, four images

of parameters are acquired and called Laguerre coefficients (LEC's). The decay curve at each pixel is used to calculate lifetime images using the 1/e average lifetime definition[4] and integrated to form intensity images. Aside from these 6 images of data from each filter, ratios of the 6 images are also created by dividing f2 into f1 images. The data in the images is quantified using histograms and based on these histograms, ranges of data in f1 and f2 images are used for our analysis as well.

2.2 Correlation with histopathology

After the samples were marked with India ink they were fixed in formalin, embedded in paraffin, and processed routinely. 4 μm segments were stained for hematoxylin and eosin (H&E) and elastin-trichrome and analyzed by a pathologist (R.S.) for percentages (0-100) of fibrosis, elastin, calcification, necrosis, cholesterol, macrophages, and lymphocytes within the 4 mm by 250 μm region of interest defined by the fiber-optic excitation-collection geometry of our FLIM system and marked by the India ink.

The images were categorized based on their histopathological analysis into three broad categories: lipid-rich (>20% necrosis, cholesterol, macrophages, and lymphocytes), collagen-rich (>60% fibrosis), and early lesion (<20% necrosis, cholesterol, macrophages, and lymphocytes, <60% fibrosis). Calcification does not fluoresce with 337 nm excitation but it is still of interest because its presence in any imaging volume will reduce the intensity of fluorescence measured there.

3. RESULTS

The resulting images were analyzed in two ways. The first was by calculating ratios of f1/f2 lifetime images and the second was calculating ratios of ranges of lifetime values between f1 and f2. See figure 1 for a more detailed explanation of these two analysis methods.

3.1 Histopathology results

Based on our pathologist's analysis, we separated our 80 images into 3 groups: lipid rich (>20% lipid and macrophage content), collagen rich (>60% collagen and <20% lipid and macrophage content), and early lesion which did not fall into the other two categories and had elastin components. 42 plaques were characterized by histopathology as lipid-rich, 28 as collagen-rich, and 10 as early-lesion.

3.2 FLIM lifetime images

FLIM lifetime images from f1 (377 nm) showed lifetimes ranging from 1.8 to 3.5 ns and images from f2 (460 nm) showed lifetimes from around 1.8 ns to 3 ns. The early lesion group was dominated by elastin fluorescence and was around 2 ns from both f1 and f2. The lipid-rich plaques showed areas of shorter lifetimes (1.8 ns in both f1 and f2) as well as longer lifetimes (3.5 ns in f1 and 3 ns in f2). Collagen-rich plaques showed consistently longer lifetimes in f1 (3-3.5 ns) and lifetimes of 2.5-3 ns in f2.

3.3 FLIM compared to plaque histopathology

In this study, we correlated average fluorescence lifetime images with histopathology. We derived two types of parameters from our dataset: FLIM-derived parameter 1) histograms of ratios of average lifetimes between f1 and f2 and FLIM-derived parameter 2) ratios of ranges of lifetimes between f1 and f2 (**see** figure 1). We compared each set of parameters separately to the three categories defined by histopathology: early lesion, lipid-rich, and collagen-rich. We found clear discrimination between the mean values of the ratio images (FLIM-derived parameter 1): early lesions: 0.9 +/- 0.05, lipid rich: 1.0+/- 0.05, and collagen rich: 1.19+/-0.05. We also found discrimination between the ratios of ranges of lifetime values (FLIM-derived parameter 2) between the collagen rich group (1.6 +/- 0.1) and the lipid rich and early lesion groups, but no clear discrimination between the early lesion and lipid rich groups for this case.

4. DISCUSSION

Our results show discrimination between the three histopathological groups: early lesion, lipid-rich, and collagen-rich based on the two FLIM-derived parameters outlined in figure 1.

4.1 Average fluorescence lifetimes of common plaque components

The fluorophores present in normal artery are elastin, collagen I, and collagen III (less than collagen I), collagen-rich plaques are collagen I (more than in normal artery) and collagen III, and in lipid-rich plaques are collagen I and III (less than in collagen-rich plaques), and lipid and inflammatory components such as LDL, cholesteryl linoleate/oleate, and lipopigments like carotenoids . **Figure 3** shows the average fluorescence lifetimes of these components[11].

4.2 Expected results from FLIM-derived parameter 1

We expect early lesions to have a fluorescence lifetime of ∼ 2 ns from f1 (377 nm) and f2 (460 nm) and the f1/f2 lifetime image ratio to be ∼ 1. For collagen-rich lesions we expect higher lifetimes from f1 ∼ 3-3.5 ns and 2.5 ns from f2 and the f1/f2 ratio to be > 1. For lipid-rich lesions we expect shorter lifetimes from both f1 and f2 and so depending on the types of lipid and inflammatory cells present, a varying f1/f2 ratio from <1 to ∼ 1.

4.3 Expected results from FLIM-derived parameter 2

We expect early lesions to have small ranges of lifetimes in both f1 (377 nm) and f2 (460 nm) and thus a ratio of these (f1/f2) ranges to be ∼1. For collagen-rich lesions we expect a larger range of values in f1 (1-1.5 ns) and a smaller range from f2 (0.5 ns) yielding a ratio of ranges ∼ 2. For lipid-rich lesions we expect a larger range of values in both f1 and f2 depending on the types of lipid and inflammatory cells present so a ratio of ranges varying from <1 to >1.

4.4 Summary of results

Results from correlating FLIM-derived parameter 1 with histopathology were closest to what we expected based on the values shown in figure 4. For example, the average ratio of

f1/f2 images was ∼ 1.2 in the collagen-rich case, greater than the ratio of ∼1 seen in the lipid-rich case. Also, the ratio of f1/f2 images in the early lesion group were a little less than 1, close to the ∼1 value we expected. Also the high value (∼1.6) of the ratios of ranges of lifetime values from the collagen-rich plaques was nearly what we expected (∼2).

What we did not expect was the inability to discriminate early lesions from lipid-rich plaques by ratios of ranges of lifetime values (FLIM-derived parameter 2). The averages of each of these groups were overlapping with the standard error of the other. Interestingly, there were 4 locations in particular in the lipid-rich group with necrotic cores. These 4 plaques had shorter lifetimes at the f2 (460 nm) range which caused the ratio of ranges to be closer to 1 and the early lesion value for this parameter than the rest of the lipid-rich plaques which mainly showed a shortening of lifetime in the f1 (377 nm) range which had ratio ranges a little greater than 1 but still less than the collagen-rich plaques (ratio of ∼ 1.2). We attribute this to lipopigments such as ceroid which fluoresce at longer wavelengths (470 nm) and have also been shown to be associated with the oxidized lipids in plaques with necrotic cores[12]. We expect that with more data, we will be able to validate this hypothesis that FLIM-derived parameters can recognize the difference in fluorescence lifetime between lipid-rich plaques with or without necrotic cores and thus a way to use FLIM-derived parameter 2 as well as 1 for discriminating between early lesions, lipid-rich, and lipid-rich lesions with necrotic cores.

5. CONCLUSIONS

This study represents the preliminary work in a project targeting the development of a method of characterizing atherosclerotic plaque composition particularly related to vulnerability in vivo. This endoscopic FLIM system is designed with a prism at the tip of the imaging bundle for side-viewing implementation to allow for intravascular potential. We are continuing to collect atherosclerotic artery specimens and improve our data processing methods to include the extra information provided by the Laguerre expansion coefficients and fluorescence intensity images. In the future we expect this method to be capable of providing a tool for studying and diagnosing vulnerable plaques in vivo.

REFERENCES

[1]. Weintraub HS. Identifying the vulnerable patient with rupture-prone plaque. American Journal of Cardiology. Jun 16.2008 101:3F–10F. [PubMed: 18243856]

[2]. Sanz J, Fayad ZA. Imaging of atherosclerotic cardiovascular disease. Nature. Feb 21.2008 451:953–957. [PubMed: 18288186]

[3]. Virmani R, Burke AP, Farb A, Kolodgie FD. Pathology of the vulnerable plaque. Journal of the American College of Cardiology. Apr 18.2006 47:C13–C18. [PubMed: 16631505]

[4]. Lakowicz, JR. Principles of Fluorescence Spectroscopy. Kluwer Academic/Plenum Publishers; New York: 1999.

[5]. Laifer LI, Obrien KM, Stetz ML, Gindi GR, Garrand TJ, Deckelbaum LI. Biochemical Basis for the Difference between Normal and Atherosclerotic Arterial Fluorescence. Circulation. Dec.1989 80:1893–1901. [PubMed: 2532078]

[6]. Marcu L, Jo JA, Fang Q, Papaioannou T, Reil T, Qiao JH, Baker JD, Freischlag JA, Fishbein M. Detection of rupture-prone atherosclerotic plaques by time-resolved laser-induced fluorescence spectroscopy. Atherosclerosis. 2008; 10552

[7]. Marcu L, Jo JA, Fang QY, Papaloannou T, Qiao JH, Fishbein MC, Baker JD, Freischlag JA. Detection of high-risk atherosclerotic plaques by time-resolved laser induced fluorescence spectroscopy. Circulation. Oct 25.2005 112:U678–U678.

[8]. Marcu L, Fishbein MC, Maarek JMI, Grundfest WS. Discrimination of human coronary artery atherosclerotic lipid-rich lesions by time-resolved laser-induced fluorescence spectroscopy. Arteriosclerosis Thrombosis and Vascular Biology. Jul.2001 21:1244–1250.

[9]. Marcu L, Fang QY, Jo JA, Papaioannou T, Dorafshar A, Reil T, Qiao JH, Baker JD, Freischlag JA, Fishbein MC. In vivo detection of macrophages in a rabbit atherosclerotic model by time-resolved laser-induced fluorescence spectroscopy. Atherosclerosis. Aug.2005 181:295–303. [PubMed: 16039283]

[10]. Jo JA, Fang QY, Papaioannou T, Marcu L. Fast model-free deconvolution of fluorescence decay for analysis of biological systems. Journal of Biomedical Optics. Jul-Aug;2004 9:743–752. [PubMed: 15250761]

[11]. Marcu, L.; Grundfest, WS.; Fishbein, M. Time-Resolved Laser-Induced Fluorescence Spectroscopy for Staging Atherosclerotic Lesions. In: Mycek, MA.; Pogue, BW., editors. Handbook of Biomedical Fluorescence. Marcel Dekker, Inc.; New York: 2003. p. 397-430.

[12]. Wen YC, Leake DS. Low density lipoprotein undergoes oxidation within lysosomes in cells. Circulation Research. May 11.2007 100:1337–1343. [PubMed: 17446432]

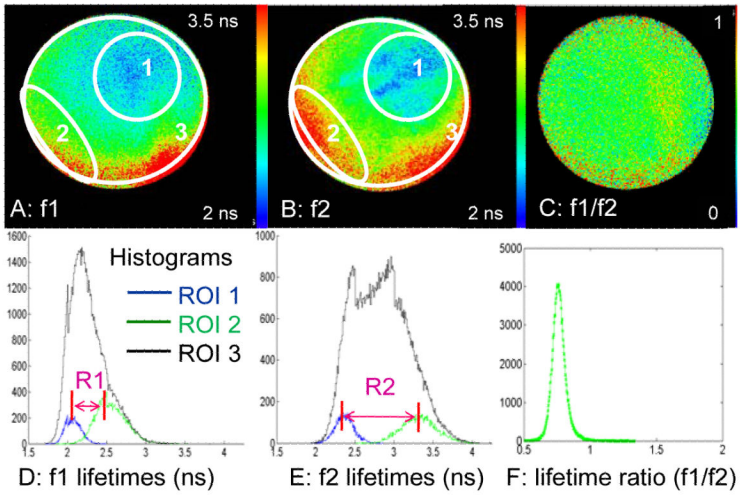

Figure 1.

A and B) Average lifetime images from filters 1 (377 nm) and 2 (460 nm). The white lines show the regions of interest (ROIs) selected for the histograms in D & E. ROI1 is the area of shortest lifetime, ROI2 the area of longest lifetime, and ROI3 the entire image. C) Ratio of images A and B. To quantify these images we calculate the ratio of ranges of lifetimes between f1 and f2. D and E) Histograms of lifetimes from f1 and f2, R1 and R2 represent the distances between the shortest and longest lifetimes in each image. For this image set, the ratios of ranges from f1 and f2 is R1/R2 ∼ 0.5. F) Histogram of the ratio image C In this case the ratio values are all less than 1

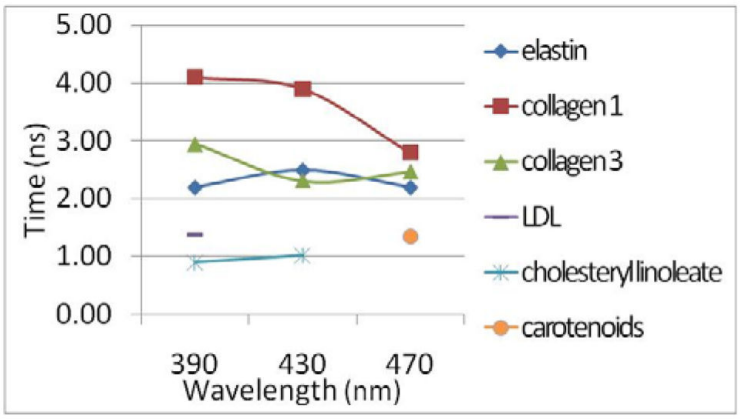

Figure 4.
Average fluorescence lifetimes of common plaque/artery components at 390, 430, and 470 nm.